Introduction to Nuclear and Particle Physics

Nuclear structure

Helga Dénes 2022 Yachay Tech

hdenes@yachaytech.edu.ec

Electron scattering

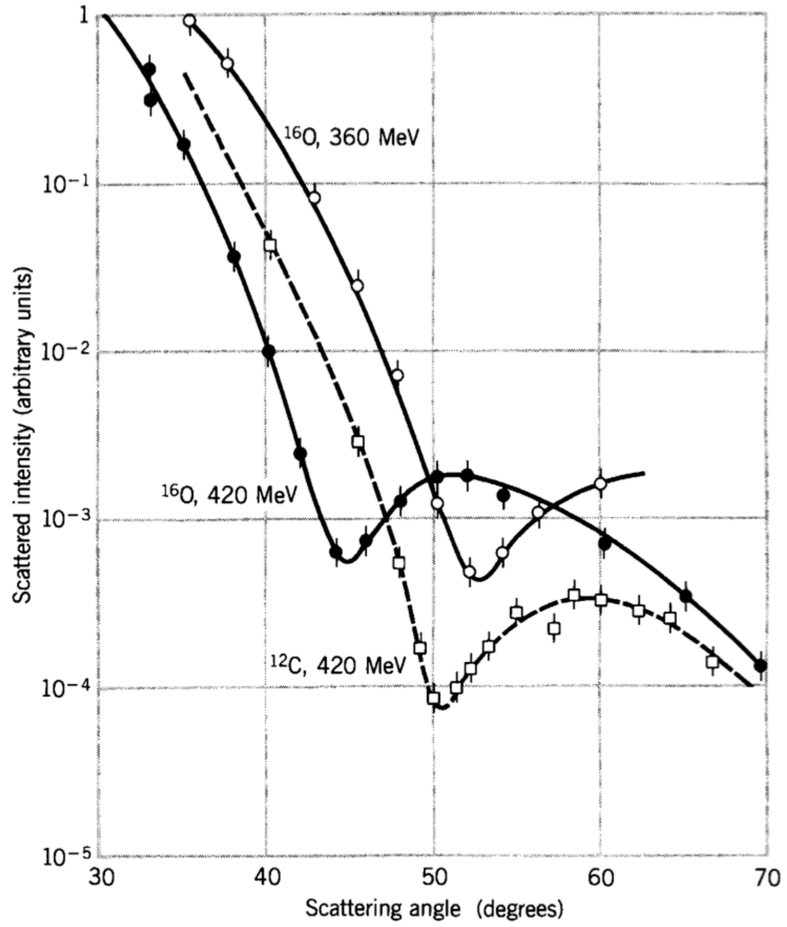

Figure 3.1 Electron scattering from ^{16}O and ^{12}C. The shape of the cross section is somewhat similar to that of diffraction patterns obtained with light waves. The data come from early experiments at the Stanford Linear Accelerator Center (H. F. Ehrenberg et al., *Phys. Rev.* **113**, 666 (1959)).

Electron scattering

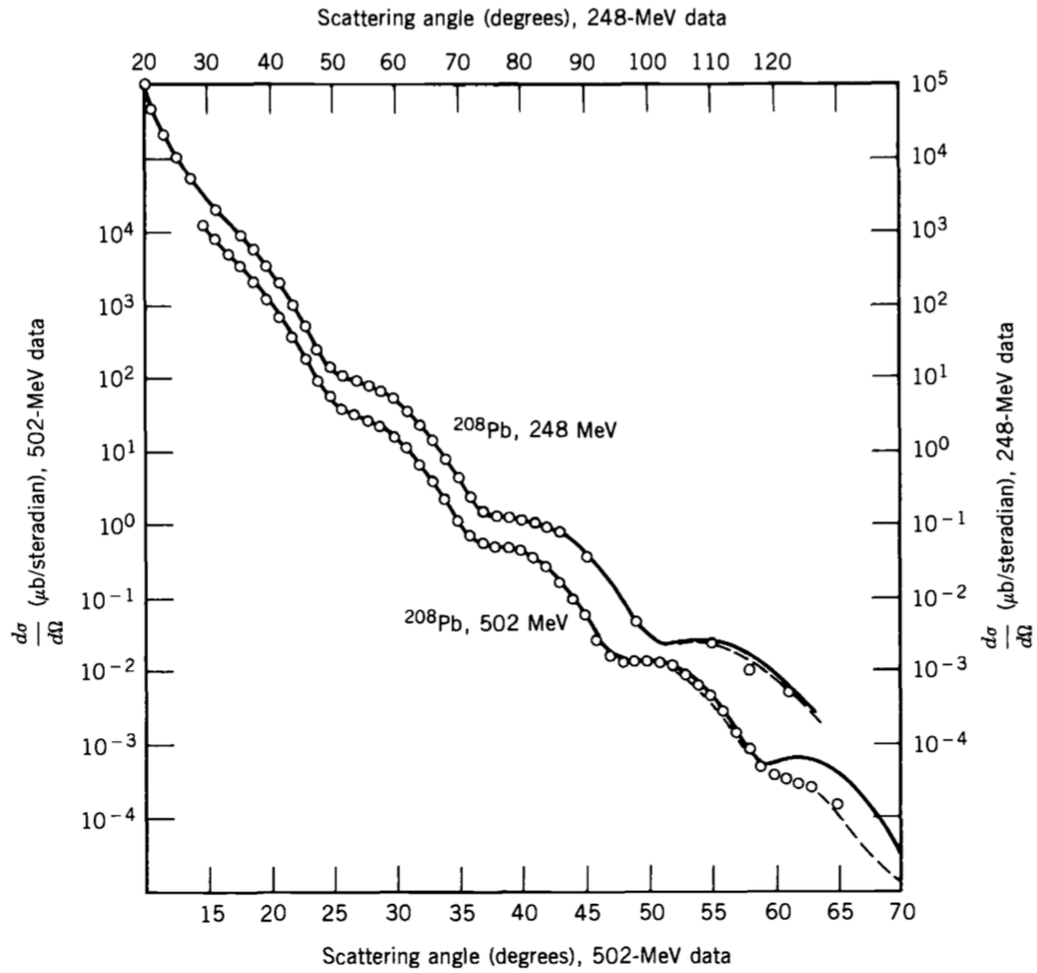

Figure 3.2 Elastic scattering of electrons from ^{208}Pb. Note the different vertical and horizontal scales for the two energies. This also shows diffractionlike behavior, but lacks sharp minima. (J. Heisenberg et al., *Phys. Rev. Lett.* **23**, 1402 (1969).)

Electron scattering

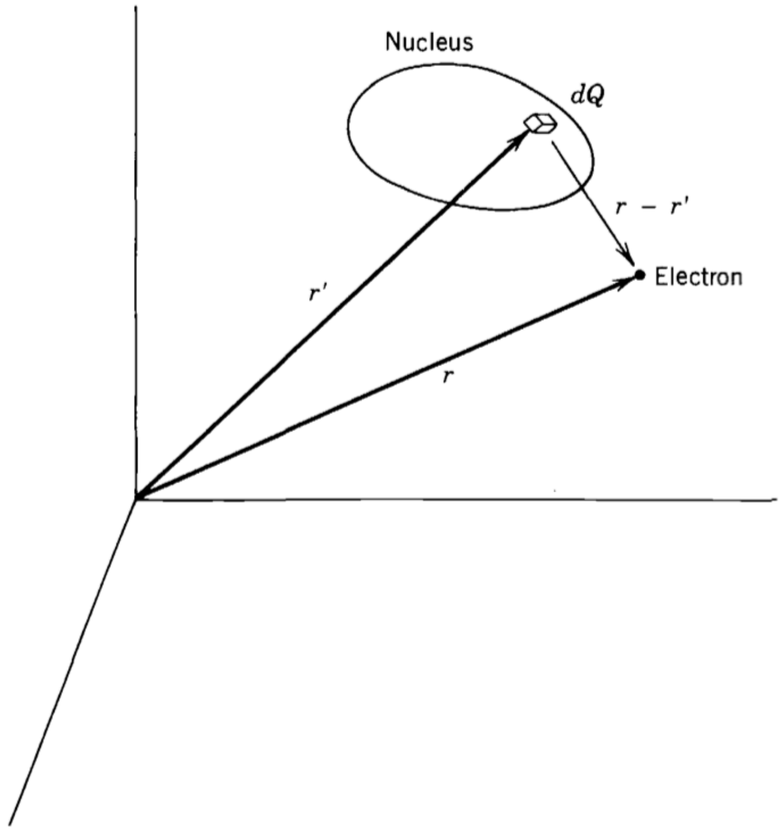

Figure 3.3 The geometry of scattering experiments. The origin of coordinates is located arbitrarily. The vector $\boldsymbol{r}'$ locates an element of charge dQ within the nucleus, and the vector $\boldsymbol{r}$ defines the position of the electron.

Electron scattering

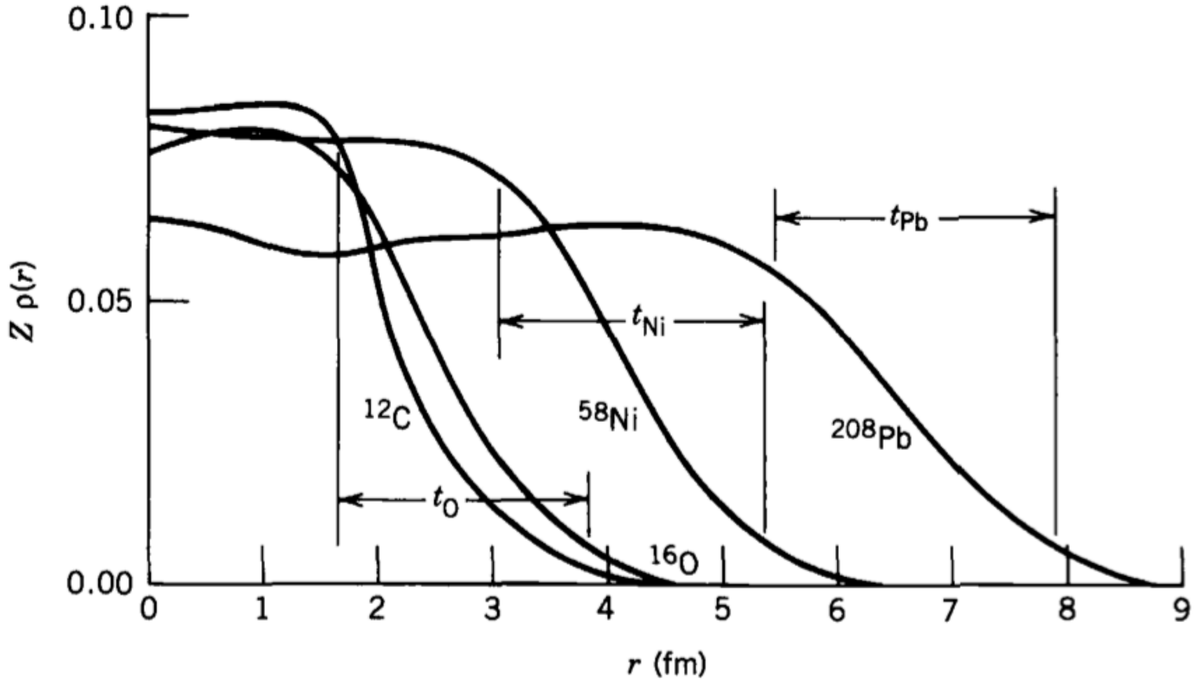

Figure 3.4 The radial charge distribution of several nuclei determined from electron scattering. The skin thickness t is shown for O, Ni, and Pb; its value is roughly constant at 2.3 fm. The central density changes very little from the lightest nuclei to the heaviest. These distributions were adapted from R. C. Barrett and D. F. Jackson, *Nuclear Sizes and Structure* (Oxford: Clarendon, 1977), which gives more detail on methods of determining $\rho(r)$.

Electron scattering

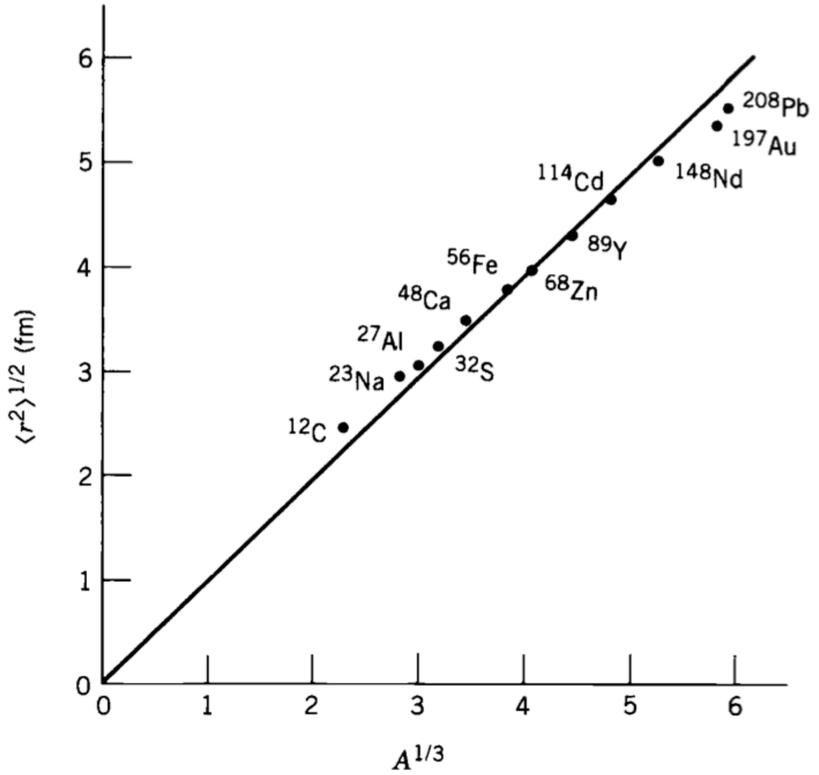

Figure 3.5 The rms nuclear radius determined from electron scattering experiments. The slope of the straight line gives $R_0 = 1.23$ fm. (The line is not a true fit to the data points, but is forced to go through the origin to satisfy the equation $R = R_0 A^{1/3}$.) The error bars are typically smaller than the size of the points (± 0.01 fm). More complete listings of data and references can be found in the review of C. W. de Jager et al., *Atomic Data and Nuclear Data Tables* **14**, 479 (1974).

Isotope shift

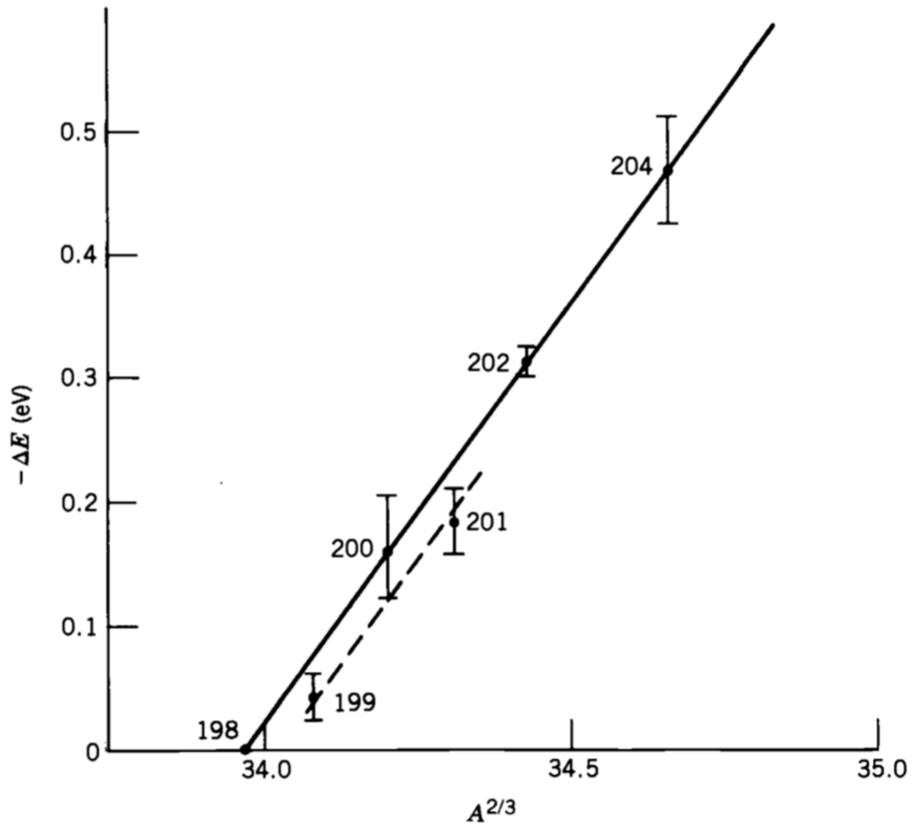

Figure 3.6 K X-ray isotope shifts in Hg. The energy of the K X ray in Hg is about 100 keV, so the relative isotope shift is of the order of 10^{-6}. The data show the predicted dependence on $A^{2/3}$. There is an "odd-even" shift in radius of odd-mass nuclei relative to their even-A neighbors, brought about by the orbit of the odd particle. For this reason, odd-A isotopes must be plotted separately from even-A isotopes. Both groups, however, show the $A^{2/3}$ dependence. The data are taken from P. L. Lee et al., *Phys. Rev. C* **17**, 1859 (1978).

Isotope shift

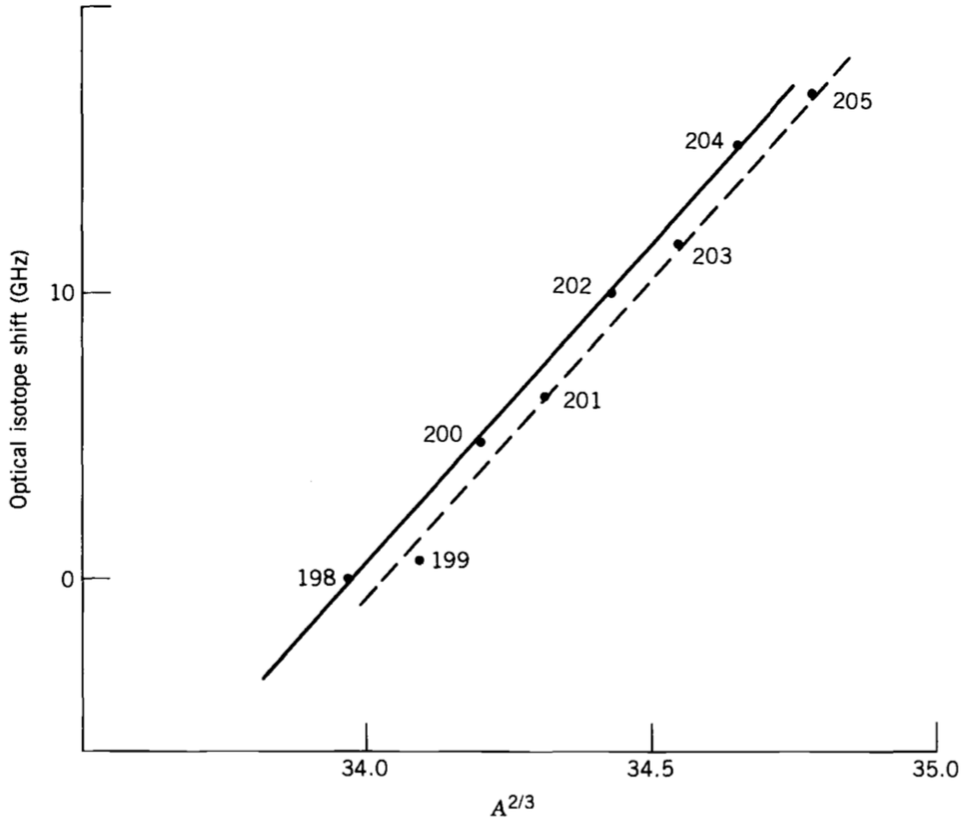

Figure 3.7 Optical isotope shifts in Hg isotopes from 198 to 205, measured relative to 198. These data were obtained through laser spectroscopy; the experimental uncertainties are about $\pm 1\%$. The optical transition used for these measurements has a wavelength of 253.7 nm, and the isotope shift is therefore about one part in 10^7. Compare these results with Figure 3.6. Data taken from J. Bonn et al., *Z. Phys. A* **276**, 203 (1976).

Isotope shift

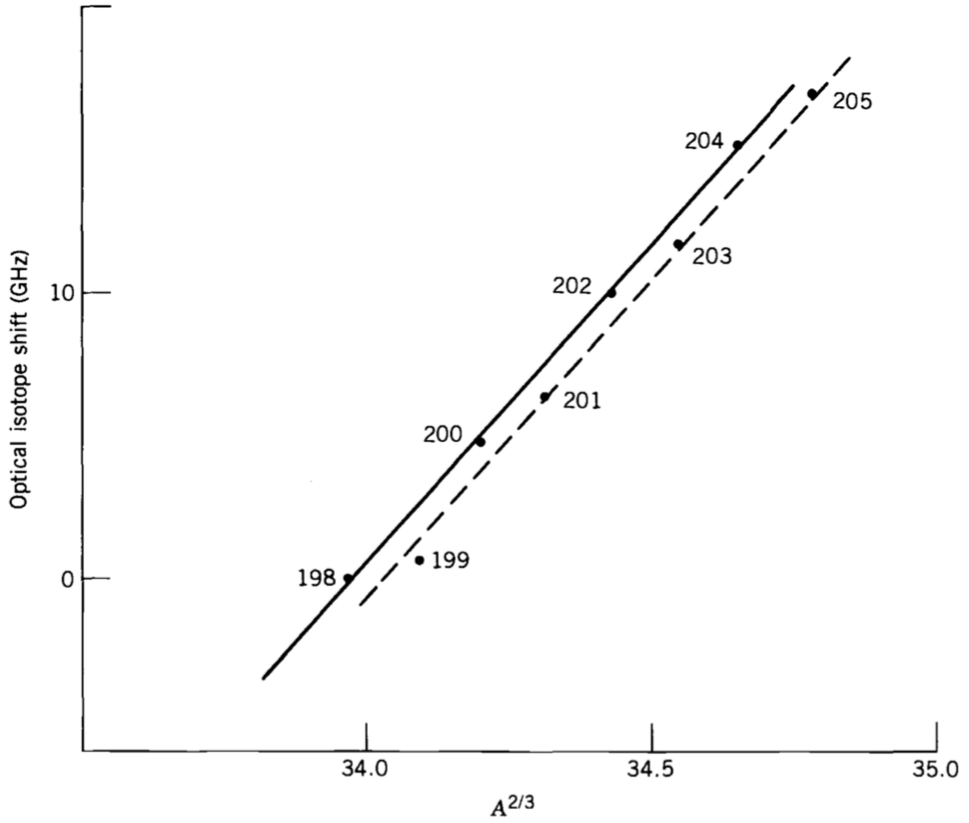

Figure 3.7 Optical isotope shifts in Hg isotopes from 198 to 205, measured relative to 198. These data were obtained through laser spectroscopy; the experimental uncertainties are about $\pm 1\%$. The optical transition used for these measurements has a wavelength of 253.7 nm, and the isotope shift is therefore about one part in 10^7. Compare these results with Figure 3.6. Data taken from J. Bonn et al., *Z. Phys. A* **276**, 203 (1976).

Isotope shift

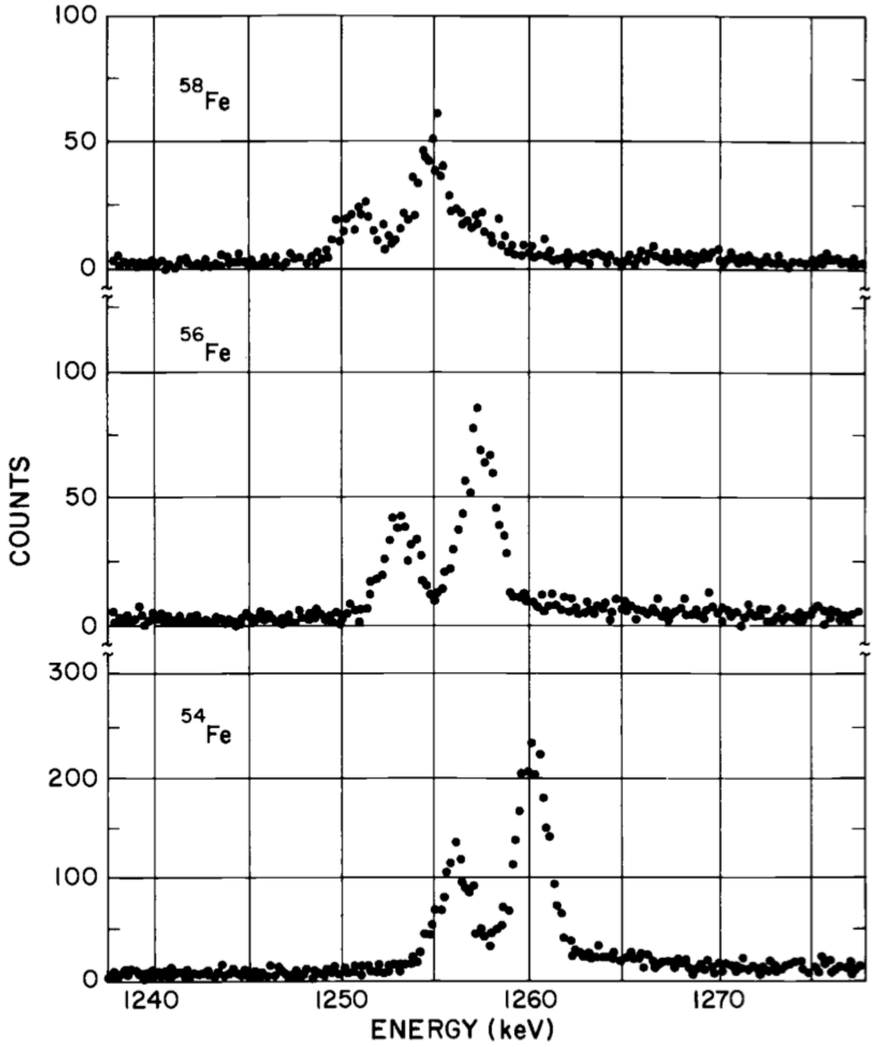

Figure 3.8 The muonic K X rays in some Fe isotopes. The two peaks show the $2p_{3/2}$ to $1s_{1/2}$ and $2p_{1/2}$ to $1s_{1/2}$ transitions, which have relative intensities in the ratio 2 : 1 determined by the statistical weight $(2j + 1)$ of the initial state. The isotope shift can clearly be seen as the change in energy of the transitions. The effect is about 0.4%, which should be compared with the 10^{-6} effect obtained with electronic K X rays (Figure 3.6). From E. B. Shera et al., *Phys. Rev. C* **14**, 731 (1976).

Isotope shift

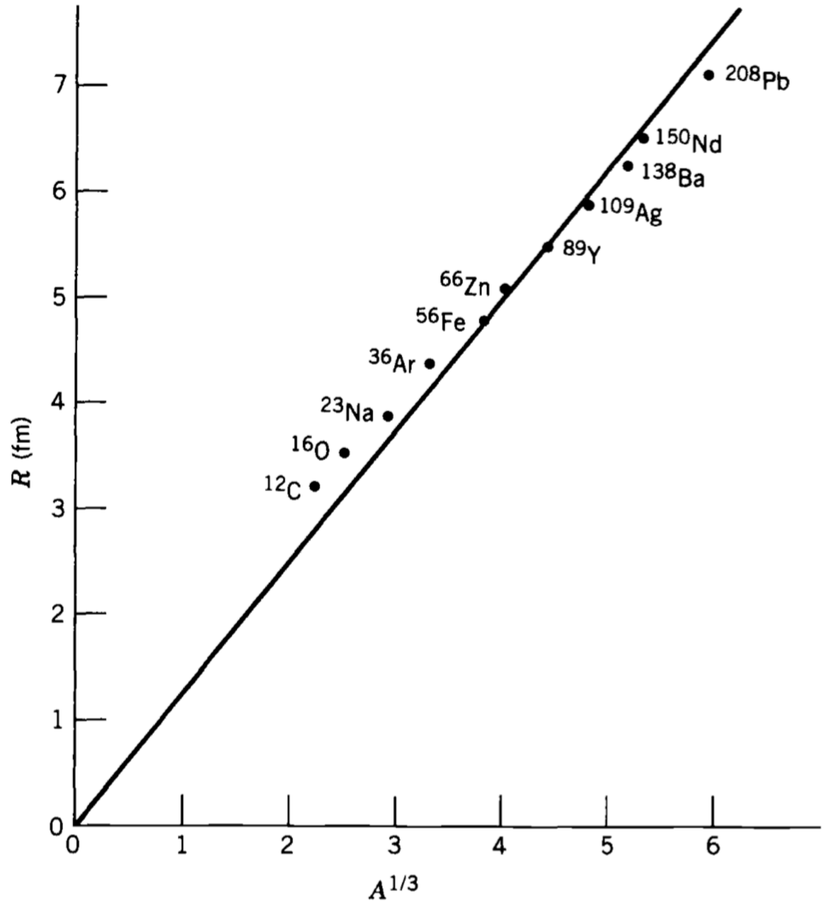

Figure 3.9 The mean nuclear radius determined from muonic X-ray measurements. As in Figure 3.5, the data depend roughly linearly on $A^{1/3}$ (again forcing the line to go through the origin). The slope of the line gives $R_0 = 1.25$ fm. The data are taken from a review of muonic X-ray determinations of nuclear charge distributions by R. Engfer et al., *Atomic Data and Nuclear Data Tables* **14**, 509 (1974).

Mirror nuclei

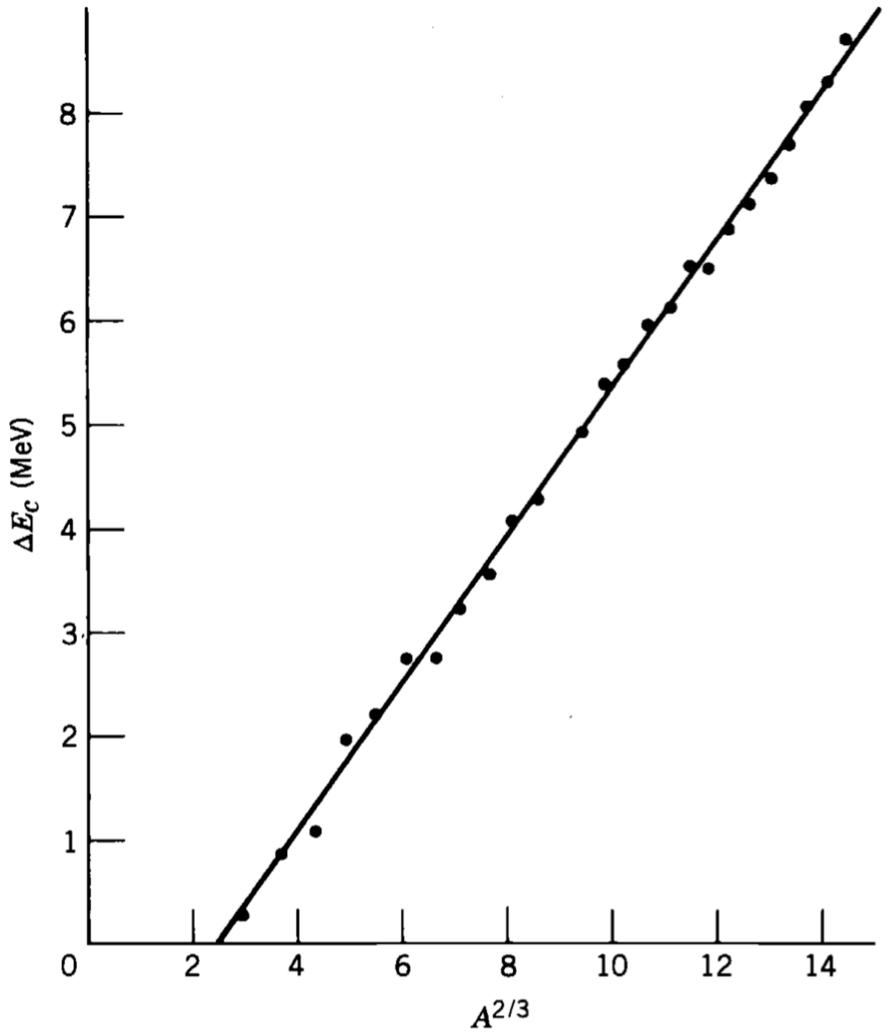

Figure 3.10 Coulomb energy differences of mirror nuclei. The data show the expected $A^{2/3}$ dependence, and the slope of the line gives $R_0 = 1.22$ fm.